Experimental Thermal and Fluid Science 35 (2011) 978–985

Contents lists available at ScienceDirect

Experimental Thermal and Fluid Science

journal homepage: www.elsevier.com/locate/etfs

The effect of vapour super-heating on hydrocarbon refrigerant condensation inside a brazed plate heat exchanger

Giovanni A. Longo *

University of Padova, Department of Management and Engineering, Str.lla S. Nicola 3, I-36100 Vicenza, Italy

ARTICLE INFO

Article history:
Received 4 November 2010
Received in revised form 30 January 2011
Accepted 30 January 2011
Available online 4 February 2011

Keywords:
Condensation
Super-heating
Refrigerant
Heat transfer
Pressure drop

ABSTRACT

This paper investigates the effect of vapour super-heating on hydrocarbon refrigerant 600a (Isobutane), 290 (Propane) and 1270 (Propylene) condensation inside a brazed plate heat exchanger.

Vapour super-heating increases heat transfer coefficient with respect to saturated vapour, whereas no effect was observed on pressure drop.

The super-heated vapour condensation data shows the same trend vs. refrigerant mass flux as the saturated vapour condensation data, but with higher absolute values. A transition point between gravity controlled and forced convection condensation has been found for a refrigerant mass flux around 15–18 kg m^{-2} s^{-1} depending on refrigerant type. The super-heated vapour heat transfer coefficients are from 5% to 10% higher than those of saturated vapour under the same refrigerant mass flux.

The experimental heat transfer coefficients have been compared against Webb (1998) model for forced convection condensation of super-heated vapour: the mean absolute percentage deviation between the experimental and calculated data is ±18.3%.

HC-1270 shows super-heated vapour heat transfer coefficient 5% higher than HC-600a and 10–15% higher than HC-290 together with total pressure drops 20–25% lower than HC-290 and 50–66% lower than HC-600a under the same mass flux.

1. Introduction

In the inverse cycle machines the refrigerant vapour coming from the compressor at the inlet of the condenser exhibits some degrees of super-heating, normally from 10 °C to 50 °C, depending on the isoentropic characteristics of the refrigerant and the pressure ratio. Therefore it is interesting, under a technical point of view, to evaluate the performance of the condenser not only in saturated vapour condensation as it is usual, but also in the real operating conditions in chiller and heat pump considering the effect of vapour super-heating.

Minkowycz and Sparrow [1,2] analytically investigated the effect of vapour super-heating both in laminar film and forced convection condensation by integrating the energy and momentum equation in the boundary layer. For steam condensation they computed a maximum heat transfer coefficient increase of 3%.

Mitrovic [3] for laminar film condensation and Webb [4] for forced convection condensation shown that the condensate film is thinner and therefore the heat transfer coefficient is larger for super-heated vapour than for saturated vapour condensation. They provided also analytical solutions accounting for super-heating effect on condensate film thickness and heat transfer coefficient.

With specific reference to refrigerant super-heated vapour condensation Goto et al. [5] measured the heat transfer coefficient during CFC-113 film condensation on a horizontal tube and they found a 5% of heat transfer coefficient enhancement with respect to saturated vapour condensation for 40 °C of super-heating. Huebesch and Pate [6] experimentally investigated HFC-236ea and CFC-114 condensation on plain and integral fin tubes and they found a 3–5% enhancement with 3–5 °C of super-heating. Longo [7,8] measured the heat transfer coefficients of HFC-134a and HFC-410A saturated and super-heated vapour (10 °C) inside a brazed plate heat exchanger. The super-heated vapour heat transfer coefficients are 8–10% higher than those of saturated vapour under the same refrigerant mass flux both for HFC-134a and HFC-410A.

The present paper investigates the effect of vapour super-heating on hydrocarbon refrigerant 600a (Isobutane), 290 (Propane) and 1270 (Propylene) condensation inside a brazed plate heat exchanger.

2. Experimental set-up and procedures

The experimental facility, as shown in Fig. 1, consists of a refrigerant loop, a water-glycol loop and two water loops. In

* Tel.: +39 0444 998726; fax: +39 0444 998888.
E-mail address: tony@gest.unipd.it

0894-1777/$ - see front matter © 2011 Elsevier Inc. All rights reserved.
doi:10.1016/j.expthermflusci.2011.01.018

Nomenclature

A	nominal area of a plate, m^2
b	height of the corrugation, m
c_p	specific heat capacity, J kg^{-1} K^{-1}
d_h	hydraulic diameter, $d_h = 2b$, m
F	factor in Eq. (12)
f.s.	full scale
g	gravity acceleration, m s^{-2}
G	mass flux, $G = m/(n_{ch}Wb)$, kg m^{-2} s^{-1}
h	heat transfer coefficient, W m^{-2} K^{-1}
J	specific enthalpy, J kg^{-1}
k	coverage factor
L	flow length of the plate, m
m	mass flow rate, kg s^{-1}
N	number of plates effective in heat transfer
n_{ch}	number of channels
p	pressure, Pa
P	corrugation pitch, m
Pr	Prandtl number, $Pr = \mu c_p/\lambda$
q	heat flux, $q = Q/S$, W m^{-2}
Q	heat flow rate, W
Ra	arithmetic mean roughness (ISO 4271/1), μm
Re	Reynolds number, $Re = Gd_h/\mu$
Re_{eq}	equivalent Reynolds number, $Re_{eq} = G[(1 - X) + X(\rho_L/\rho_G)^{1/2}]d_h/\mu_L$
R_p	roughness (DIN 4762/1), μm
s	plate wall thickness, m
S	nominal heat transfer area, m^2
T	temperature, K
U	overall heat transfer coefficient, W m^{-2} K^{-1}
v	specific volume, m^3 kg^{-1}
V	volume, m^3
W	width of the plate, m
X	vapour quality, $X = (J - J_L)/\Delta J_{LG}$

Greek symbols

β	inclination angle of the corrugation
Δ	difference
ΔJ_{LG}	latent heat of condensation (vaporisation), J kg^{-1}
ϕ	enlargement factor
λ	thermal conductivity, W m^{-1} K^{-1}
μ	viscosity, kg m^{-1} s^{-1}
ρ	density, kg m^{-3}

Subscripts

ave	average
AKERS	Akers et al. [18]
e	evaporator
eq	equivalent
fc	forced convection
G	vapour phase
in	inlet
L	liquid phase
LG	liquid gas phase change
lat	latent
ln	logarithmic
m	average value
out	outlet
p	plate
r	refrigerant
t	total
sat	saturation
sup	super-heating
w	water
wall	tube or plate wall
wi	water inlet
wo	water outlet

the first loop the refrigerant is pumped from the sub-cooler into the evaporator where it is evaporated and eventually super-heated to achieve the set vapour quality or vapour super-heating at the condenser inlet. The refrigerant goes through the condenser where it is condensed and eventually sub-cooled and then it comes back to the post-condenser and the sub-cooler. A variable speed volumetric pump varies the refrigerant flow rate and a bladder accumulator, connected to a nitrogen bottle and a pressure regulator, controls the operating pressure in the refrigerant loop. The second loop is able to supply a water-glycol flow at a constant temperature in the range of −10 to 60 °C with stability within ±0.1 K used to feed the sub-cooler and the post-condenser. The third and the fourth loops supply two water flows at a constant temperature in the range of 3–60 °C with stability within ±0.1 K used to feed the evaporator and the condenser respectively.

The condenser tested is a BPHE consisting of 10 plates, 72 mm in width and 310 mm in length, which present a macro-scale herringbone corrugation with an inclination angle of 65° and a corrugation amplitude of 2 mm. Fig. 2 and Table 1 give the main geometrical characteristics of the BPHE tested.

The temperatures of refrigerant and water at the inlet and outlet of the condenser and the evaporator are measured by T-type thermocouples (uncertainty ($k = 2$) within ±0.1 K); the water temperature variations through the condenser and the evaporator are measured by T-type thermopiles (uncertainty ($k = 2$) within ±0.05 K). The refrigerant pressures at the inlet of the condenser and the evaporator are measured by two absolute strain-gage pressure transducers (uncertainty ($k = 2$) within 0.075% f.s.); the refrigerant pressure drop through the condenser is measured by a strain-gage differential pressure transducer (uncertainty ($k = 2$) within 0.075% f.s.). The refrigerant mass flow rate is measured by means of a Coriolis effect mass flow meter (uncertainty ($k = 2$) of 0.1% of the measured value); the water flow rates through the condenser and the evaporator are measured by means of magnetic flow meters (uncertainty ($k = 2$) of 0.15% of the f.s.). All the measurements are scanned and recorded by a data logger linked to a PC: Table 2 outlines the main features of the different measuring devices in the experimental rig.

Before starting each test the refrigerant is re-circulated through the circuit, the post-condenser and the sub-cooler are fed with a water-glycol flow rate at a constant temperature and the condenser and the evaporator are fed with water flow rates at constant temperatures. The refrigerant pressure and the vapour quality or super-heating at the condenser inlet and outlet are controlled by adjusting the bladder accumulator, the volumetric pump, the flow rate and the temperature of the water glycol and the water flows. Once temperature, pressure, flow rate and vapour quality steady state conditions are achieved at the condenser inlet and outlet both on refrigerant and water sides all the readings are recorded for a set time and the average value during this time is computed for each parameter recorded.

Super-heated vapour condensation is a complex phenomenon, particularly inside BPHE, due to the complicated geometry and the inaccessibility of the heat transfer surface. Therefore the experimental results are reported in terms of average heat transfer coefficient and total pressure drop on the refrigerant side.

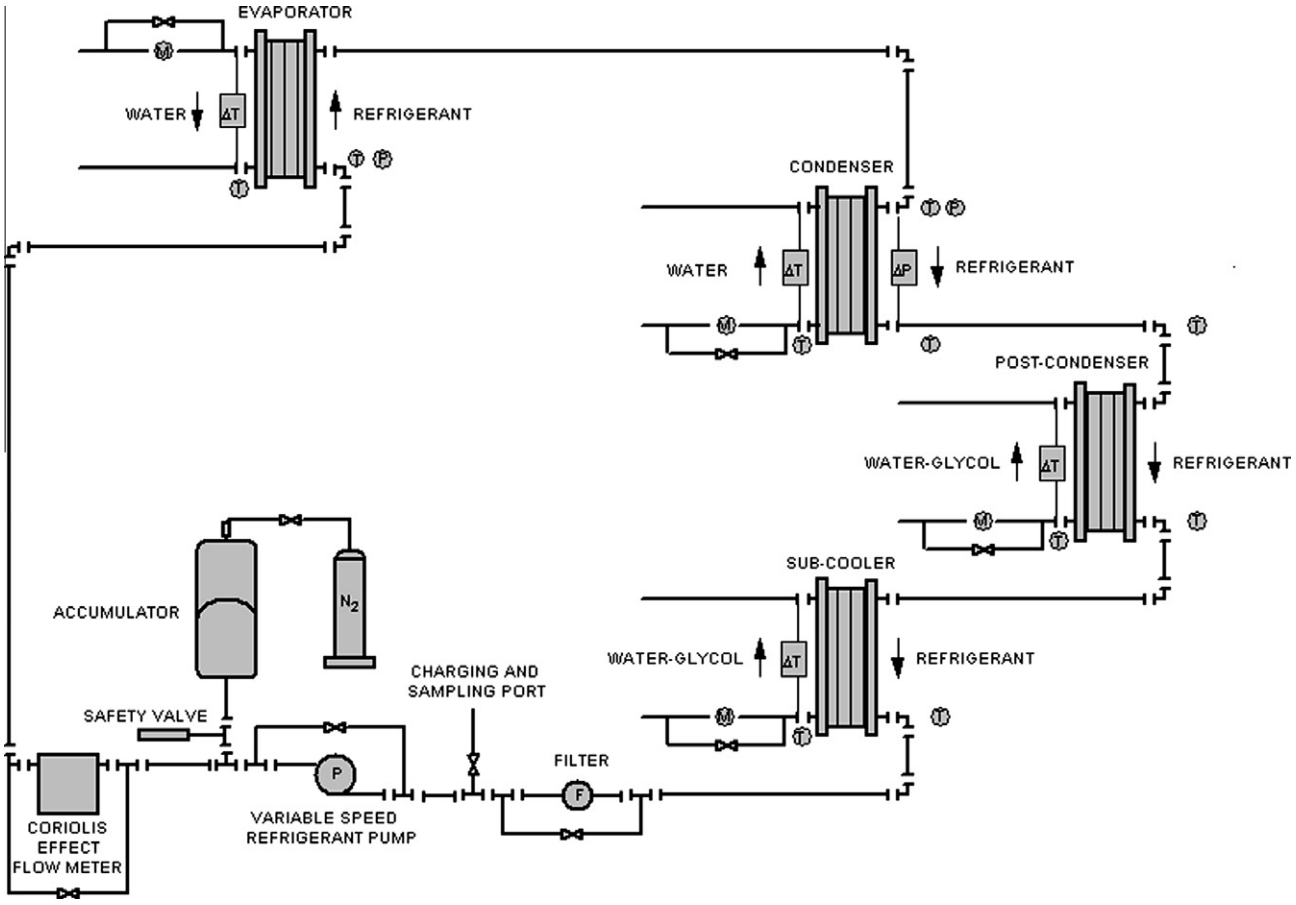

Fig. 1. Schematic view of the experimental test rig.

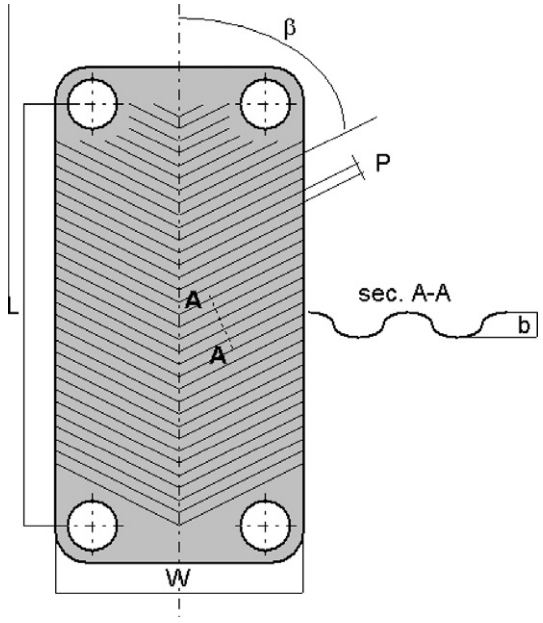

Fig. 2. Schematic view of the plate.

The overall heat transfer coefficient in the condenser U is equal to the ratio between the heat flow rate Q, the nominal heat transfer area S and the logarithmic mean temperature difference ΔT_{ln}

Table 1
Geometrical characteristics of the condenser.

Fluid flow plate length L (mm)	278.0
Plate width W (mm)	72.0
Area of the plate A (m^2)	0.02
Enlargement factor Φ	1.24
Corrugation type	Herringbone
Angle of the corrugation β (°)	65
Corrugation amplitude b (mm)	2.0
Corrugation pitch P (mm)	8.0
Plate roughness R_a (μm)	0.4
Plate roughness R_p (μm)	1.0
Number of plates	10
Number of plates effective in heat transfer N	8
Number of channels on refrigerant side $n_{ch.r}$	4
Number of channels on water side $n_{ch.w}$	5

$$U = Q/(S\Delta T_{ln}) \tag{1}$$

The heat flow rate is derived from a thermal balance on the waterside of the condenser:

$$Q = m_w c_{pw} |\Delta T_w| \tag{2}$$

where m_w is the water flow rate, c_{pw} the water specific heat capacity and $|\Delta T_w|$ the absolute value of the temperature variation on the waterside of the condenser. It includes both the desuper-heating and the phase change contributions. The nominal heat transfer area of the condenser

$$S = NA \tag{3}$$

Table 2
Specification of the different measuring devices.

Devices	Type	Uncertainty ($k = 2$)	Range
Thermometers	T-type thermocouples	0.1 K	−20/80 °C
Diff. thermometers	T-type thermopiles	0.05 K	−20/80 °C
Abs.pressure transd.	Strain-gage	0.075% f.s.	0/2.5 MPa
Diff. pressure transd.	Strain-gage	0.075% f.s.	0/0.3 MPa
Refrigerant flow meter	Coriolis effect	0.1%	0/300 kg h^{-1}
Water flow meters	Magnetic	0.15% f.s.	100/1200 l h^{-1}

is equal to the nominal projected area $A = L \times W$ of the single plate multiplied by the number N of the effective elements in heat transfer. The use of the projected area instead of the actual area allows comparing different plate patterns on an equal volume basis, as suggested by Shah and Focke [9]. Moreover, due to the brazing material deposition, the actual heat transfer area of a BPHE is different from that of the plates and generally unknown. The logarithmic mean temperature difference is equal to:

$$\Delta T_{ln} = (T_{wo} - T_{wi})/ln[(T_{sat} - T_{wi})/(T_{sat} - T_{wo})] \quad (4)$$

where T_{sat} is the average saturation temperature of the refrigerant derived from the average pressure measured on refrigerant side and T_{wi} and T_{wo} the water temperatures at the inlet and the outlet of the condenser. The logarithmic mean temperature difference is computed with reference to the average saturation temperature on the refrigerant side as recommended by Bell [10,11] for a proper design in super-heated vapour condensation whenever the temperature of the heat transfer surface is below the saturation temperature. In fact, if the temperature of the heat transfer surface is below the saturation temperature, the super-heated vapour condenses directly with a heat transfer coefficient near to that of saturated vapour condensation and there is no desuper-heating area at the inlet of the condenser working only with gas single-phase heat transfer coefficient. Similarly the condensate film along the whole heat transfer surface is sub-cooled and there is no sub-cooling area at the outlet of the condenser working only with liquid single-phase heat transfer coefficient. In this case, for Bell [10,11], it is both simpler and more conservative to assume that condensation will occur directly from the super-heated vapour using the saturation temperature as the temperature driving force and the average condensation heat transfer coefficient along the whole heat transfer surface, of course including the desuper-heating sensible heat in the total heat load.

The average heat transfer coefficient on the refrigerant side of the condenser $h_{r.ave}$ is derived from the global heat transfer coefficient U assuming no fouling resistances:

$$h_{r.ave} = (1/U - s/\lambda_p - 1/h_w)^{-1} \quad (5)$$

by computing the waterside heat transfer coefficient h_w using a modified Wilson plot technique. A specific set of experimental water-to-water tests is carried out on the condenser to determine the calibration correlation for heat transfer on the waterside, in accordance with Muley and Manglik [12]; the detailed description of this procedure is reported in [13].

The calibration correlation for waterside heat transfer coefficient obtained results:

$$h_w = 0.277(\lambda_w/d_h)\mathrm{Re}_w^{0.766}\mathrm{Pr}_w^{0.333} \quad (6)$$

$$5 < \mathrm{Pr}_w < 10 \quad 200 < \mathrm{Re}_w < 1200$$

The refrigerant vapour quality at the condenser inlet and outlet X_{in} and X_{out} are computed starting from the refrigerant temperature $T_{e.in}$ and pressure $p_{e.in}$ at the inlet of the evaporator (sub-cooled liquid condition) considering the heat flow rate exchanged in the evaporator and in the condenser Q_e and Q and the pressure at the inlet and outlet p_{in} and p_{out} of the condenser as follows:

$$X_{in} = f(J_{in}, p_{in}) \quad (7)$$

$$X_{out} = f(J_{out}, p_{out}) \quad (8)$$

$$J_{in} = J_{e.in}(T_{e.in}, p_{e.in}) + Q_e/m_r \quad (9)$$

$$J_{out} = J_{in} + Q/m_r \quad (10)$$

$$Q_e = m_{e.w}c_{pw}|\Delta T_{e.w}| \quad (11)$$

where J is the specific enthalpy of the refrigerant, m_r the refrigerant mass flow rate, $m_{e.w}$ the water flow rate and $|\Delta T_{e.w}|$ the absolute value of the temperature variation on the waterside of the evaporator. The refrigerant properties are evaluated by Refprop 7.0 (NIST [14]).

3. Analysis of the results

Three different sets of super-heated vapour condensation tests with refrigerant down-flow and water up-flow are carried out at four different saturation temperatures: 25, 30, 35 and 40 °C. The condenser outlet condition is slightly sub-cooled condensate. The first set includes 37 runs with HC-600a, the second 39 runs with HC-290, the third 36 runs with HC-1270. Table 3 indicates the operating conditions in the condenser under experimental tests: refrigerant saturation temperature T_{sat} and pressure p_{sat}, inlet vapour super-heating ΔT_{sup} and outlet condensate sub-cooling ΔT_{sub}, mass flux on refrigerant side G_r and water side G_w, heat flux q. The water and refrigerant mass flux and the heat flux tested cover the real operating conditions of BPHE condensers in chiller and heat pump applications [15].

A detailed error analysis performed in accordance with Kline and McClintock [16] indicates an overall uncertainty ($k = 2$) within ±12% for the refrigerant heat transfer coefficient measurement and within ±23% for the refrigerant total pressure drop measurement. Table 4 shows a summary of the uncertainty analysis.

Figs. 3–5 show the average heat transfer coefficients on the refrigerant side vs. refrigerant mass flux at different saturation temperatures (25, 30, 35 and 40 °C) for refrigerant HC-600a, HC-290 and HC-1270 respectively. For comparison the figures show also the experimental data relative to saturated vapour condensation inside the same BPHE under the same operating conditions previously obtained by the same author [17].

The heat transfer coefficients show weak sensitivity to saturation temperature (pressure) for all the refrigerants tested.

The saturated vapour data and the super-heated vapour data show the same trend vs. refrigerant mass flux for all the refrigerants tested. At low refrigerant mass flux (G_r < 15–18 kg m^{-2} s^{-1}) the heat transfer coefficients are not dependent on mass flux and probably condensation is controlled by gravity. For higher refrigerant mass flux (G_r > 15–18 kg m^{-2} s^{-1}) the heat transfer coefficients depend on mass flux and forced convection condensation occurs. In the forced convection condensation region the heat transfer coefficients show a 35–40% enhancement for a 60% increase of the refrigerant mass flux. The behaviour of the heat transfer coefficient vs. the refrigerant mass flux might be explained by considering the combined effect of gravity and vapour shear on condensate drainage. At low refrigerant mass flux (G_r < 15–18 kg m^{-2} s^{-1}) the vapour shear has a weak effect on the condensate flow which is governed mainly by gravity. For higher refrigerant mass flux (G_r > 15–18 kg m^{-2} s^{-1}) the vapour shear reduces the thickness of

Table 3
Operating conditions during experimental tests.

Set	Fluid	Runs	T_{sat} (°C)	p_{sat} (MPa)	ΔT_{sup} (K)	ΔT_{sub} (K)	G_r (kg m^{-2} s^{-1})	G_w (kg m^{-2} s^{-1})	q (kW m^{-2})
1st	HC-600a	37	25.0–40.2	0.35–0.53	9.3–10.9	0.6–3.8	7.3–28.3	68.6–327.3	9.3–35.2
2nd	HC-290	39	24.8–40.1	0.94–1.37	9.5–10.3	0.8–3.5	6.2–27.9	67.9–317.8	7.8–34.8
3rd	HC-1270	36	25.0–40.2	1.15–1.65	9.4–10.4	1.0–3.5	7.4–27.6	74.6–300.3	9.3–35.1

Table 4
Summary of the uncertainty ($k = 2$) analysis.

Variables	Maximum uncertainty ($k = 2$)
Measurements	
Water temperature T_w	±0.1 K
Water temperature difference ΔT_w	±0.05 K
Absolute pressure p_{sat}	±1.875 kPa
Differential pressure Δp	±0.225 kPa
Water flow rate m_w	±0.0005 kg s^{-1}
Refrigerant flow rate m_r	±0.1%
Geometrical parameters	
Plate length L and width W	$\pm 1 \times 10^{-3}$ m
Heat transfer area S	±1.5%
Heat transfer and pressure drop parameters	
Heat flow rate Q	±2.5%
Vapour quality X	±0.03
Overall heat transfer coefficient U	±6.7%
Water heat transfer coefficient h_w	±10.0%
Refrigerant heat transfer coefficient h_r	±12.0%
Total pressure drop Δp_t	±23.0%

the condensate film and promotes the turbulence in the condensate film increasing the heat transfer coefficient. In this region the condensate flow is governed both by gravity and vapour shear.

HC-290 super-heated vapour heat transfer coefficients are from 7% to 10% higher than those of saturated vapour, whereas HC-600a and HC-1270 show a heat transfer enhancement due to superheating from 5% to 9% under the same refrigerant mass flux.

These experimental results for HC refrigerants are consistent with those previously obtained by the same author for HFC-134a and HFC-410A [7,8].

HC-1270 shows super-heated heat transfer coefficient 5% higher than HC-600a and 10–15% higher than HC-290 under the same refrigerant mass flux. This can be attributed mainly to the higher liquid thermal conductivity of HC-1270 with respect to HC-600a and HC-290 and to the higher liquid density of HC-600a with respect to HC-1270 and HC-290.

The super-heated vapour condensation heat transfer coefficients in forced convection condensation regime ($G_r > 15$–18 kg m^{-2} s^{-1}) have been compared against the model developed by Webb [4]. Webb [4] proposed the following model to calculate the local heat transfer coefficient during forced convection condensation of super-heated vapour:

$$h_{sup} = h_{sat} + F[h_{fc} + c_{pG} q_{lat} / \Delta J_{LG}] \tag{12}$$

where h_{sat} is the local heat transfer coefficient for forced convection condensation of saturated vapour, h_{fc} is the local single-phase heat transfer coefficient between super-heated vapour and the condensate interface, c_{pG} is the specific heat capacity of the super-heated vapour, ΔJ_{LG} is the latent heat of condensation, q_{lat} is the local heat flux due only to phase change and F a factor equal to the ratio between the local degrees of super-heating and the driving temperature difference

$$F = (T_{sup} - T_{sat}) / (T_{sat} - T_{wall}) \tag{13}$$

The F factor approaches zero as the super-heating is depleted. The group $c_{pv} q_{lat} / \Delta J_{LG}$ is a correction term which accounts for the effect of mass transfer on sensible heat transfer between super-heated vapour and condensate interface. The super-heated vapour condensation heat transfer coefficient h_{sup} is referred to the temperature difference between average saturation temperature T_{sat} and average wall temperature T_{wall}.

This model may be applied to different type of condenser by using the appropriate correlations to compute the saturated vapour condensation heat transfer coefficient h_{sat} and the single-phase heat transfer coefficient h_{fc}.

In the present paper the saturated vapour condensation heat transfer coefficient has been calculated by Akers et al. [18] equation for forced convection condensation inside tube:

$$h_{AKERS} = 5.03(\lambda_L / d_h) \mathrm{Re}_{eq}^{1/3} \mathrm{Pr}_L^{1/3} \tag{14}$$

$$\mathrm{Pr}_L = \mu_L c_{pL} / \lambda_L \tag{15}$$

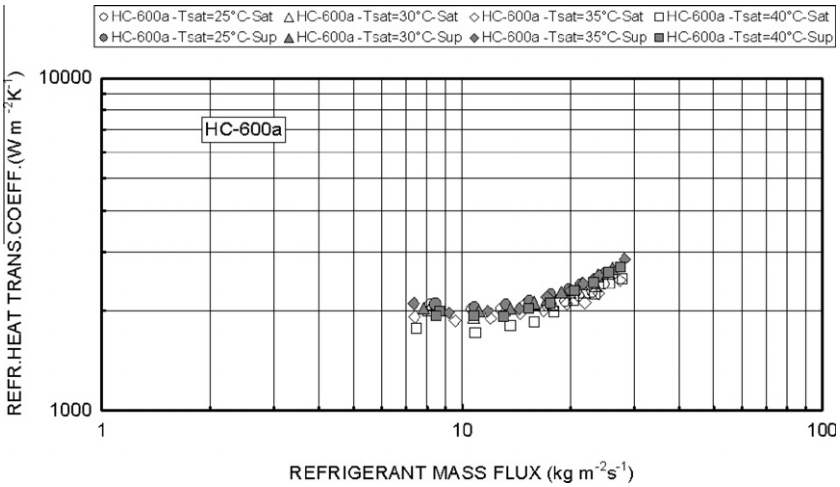

Fig. 3. Average heat transfer coefficient on refrigerant side vs. refrigerant mass flux: HC-600a.

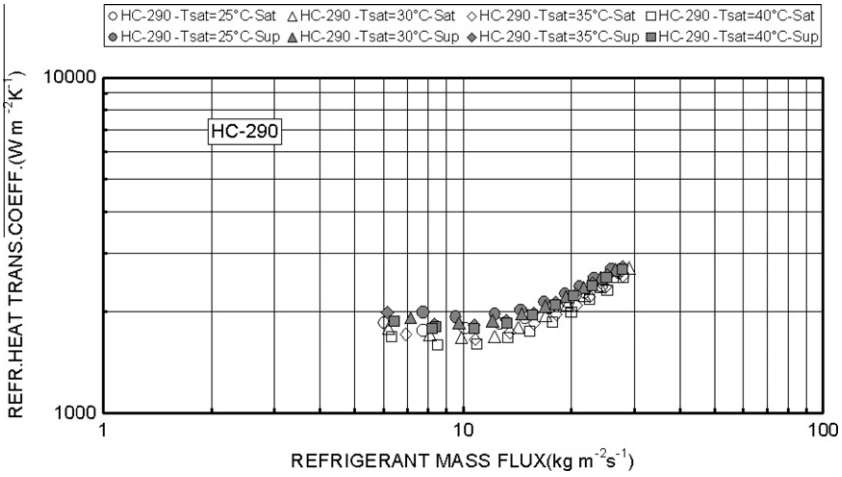

Fig. 4. Average heat transfer coefficient on refrigerant side vs. refrigerant mass flux: HC-290.

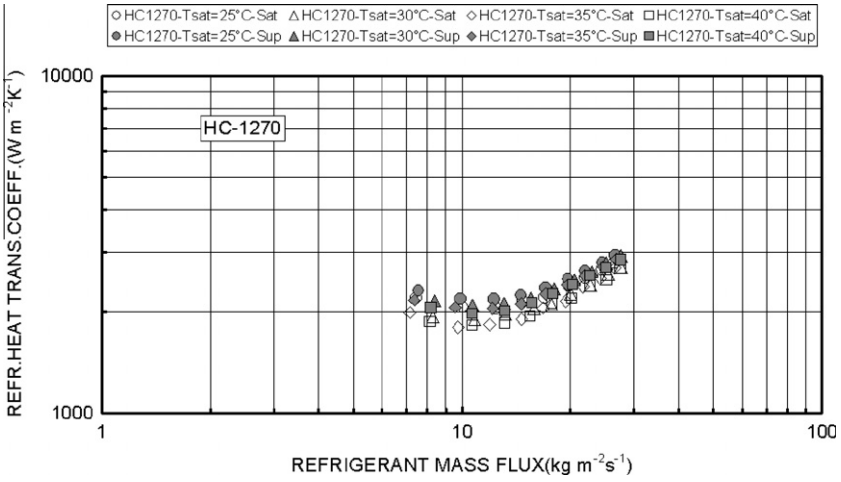

Fig. 5. Average heat transfer coefficient on refrigerant side vs. refrigerant mass flux: HC-1270.

$$\mathrm{Re}_{eq} = G\left[(1-X) + X(\rho_L/\rho_G)^{1/2}\right] d_h/\mu_L \tag{16}$$

where Pr_L and Re_{eq} are the liquid Prandtl Number and the equivalent Reynolds number. The original Akers et al. [18] equation has been multiplied by the enlargement factor Φ (equal to the ratio between the actual area and the projected area of the plates) to compute the saturated vapour condensation local heat transfer coefficient inside the BPHE referred to the projected area of the plates:

$$h_{sat} = \Phi h_{AKERS} \tag{17}$$

The local single-phase heat transfer coefficient is computed by the Thonon [19] equation:

$$h_{fc} = 0.2267(\lambda_G/d_h)\mathrm{Re}_G^{0.631}\mathrm{Pr}_G^{1/3} \tag{18}$$

$$50 < \mathrm{Re}_G < 15{,}000$$

The Webb [4] model gives the local heat transfer coefficient which has been integrated by a finite difference approach along the heat transfer area to compute the average condensation heat transfer coefficient inside the BPHE:

$$h_{r.ave} = (1/S)\int_0^S h_{sup}\, dS \tag{19}$$

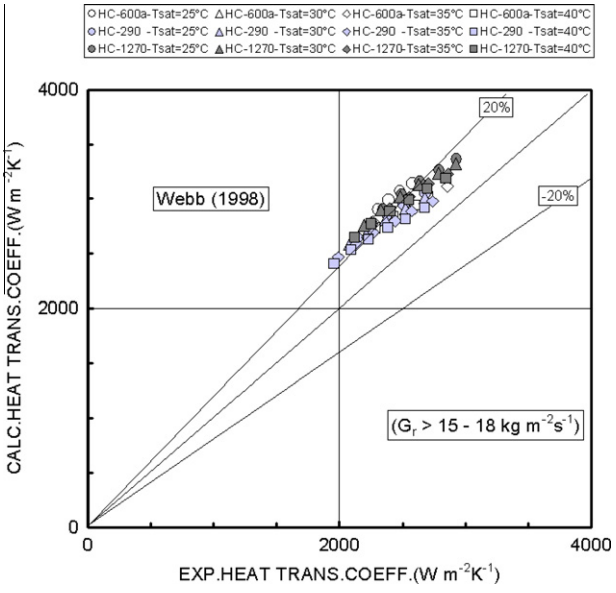

Fig. 6. Comparison between experimental and calculated heat transfer coefficients: Webb (1998) vs. experimental data with G_r > 15–18 kg m^{-2} s^{-1}.

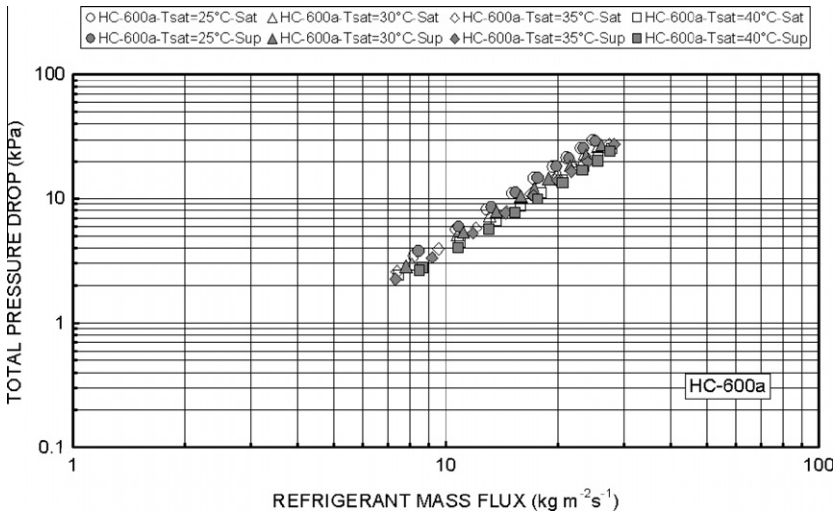

Fig. 7. Total pressure drop vs. refrigerant mass flux: HC-600a.

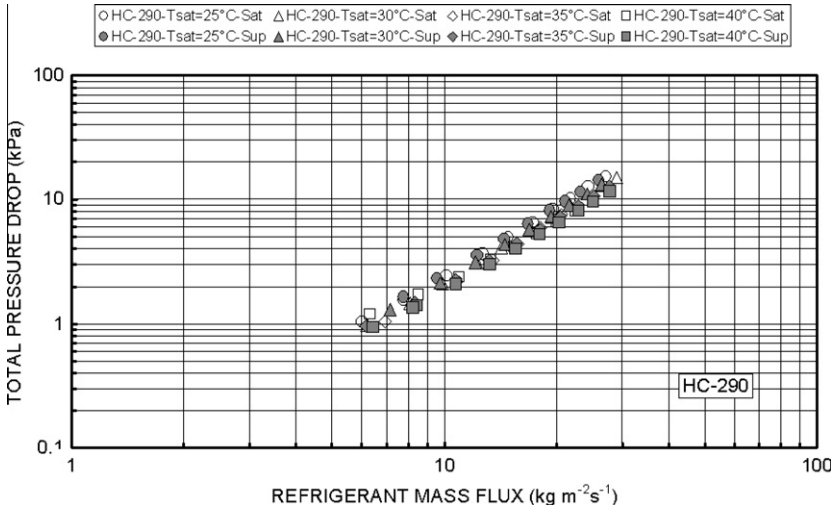

Fig. 8. Total pressure drop vs. refrigerant mass flux: HC-290.

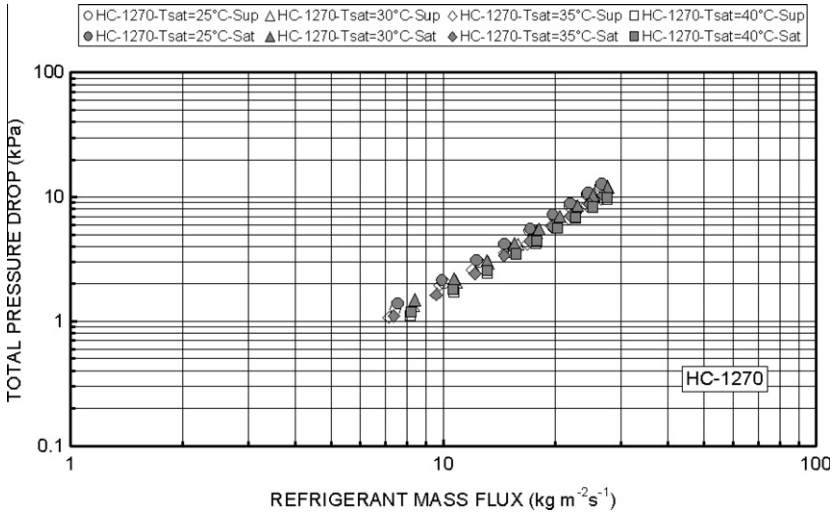

Fig. 9. Total pressure drop vs. refrigerant mass flux: HC-1270.

Fig. 6 shows the comparison between the super-heated vapour condensation heat transfer coefficients under forced convection condensation (G_r > 15–18 kg/m^2 s) and the average heat transfer coefficients calculated by Webb [4] model (Eq. (19)): the absolute mean percentage deviation is 18.3%.

Figs. 7–9 show the total pressure drop of HC-600a, HC-290 and HC-1270 at different saturation temperatures (25, 30, 35 and 40 °C) vs. the refrigerant mass flux. For comparison the figures show also the experimental data relative to saturated vapour condensation inside the same BPHE under the same operating conditions previously obtained by the same author [17]. The super-heated vapour shows total pressure drop identical to the saturated vapour under the same refrigerant mass flux for all the refrigerants and the operating conditions tested.

HC-1270 shows super-heated vapour total pressure drops 20–25% lower than HC-290 and 50–66% lower than HC-600a under the same mass flux. This can be attributed mainly to the higher reduced pressure and the lower liquid dynamic viscosity of HC-1270 with respect to HC-600a and HC-290.

4. Conclusions

This paper investigates the effect of vapour super-heating on HC refrigerant condensation inside a BPHE.

Vapour super-heating increases heat transfer coefficients with respect to saturated vapour, whereas no effects were observed on total pressure drop.

The super-heated vapour condensation data shows the same trend vs. refrigerant mass flux as the saturated vapour condensation data. A transition point between gravity controlled and forced convection condensation has been found for a refrigerant mass flux around 15–18 kg m^{-2} s^{-1} depending on refrigerant type.

HC-290 super-heated vapour heat transfer coefficients are from 7% to 10% higher than those of saturated vapour, whereas HC-600a and HC-1270 show a heat transfer enhancement from 5% to 9%.

HC-1270 shows super-heated heat transfer coefficient 5% higher than HC-600a and 10–15% higher than HC-290 together with total pressure drops 20–25% lower than HC-290 and 50–66% lower than HC-600a under the same mass flux.

References

[1] W.J. Minkowycz, E.M. Sparrow, Condensation heat transfer in presence of noncondensables, interfacial resistance, superheating, variable properties, and diffusion, Int. J. Heat Mass Transfer 9 (1966) 1125–1144.
[2] W.J. Minkowycz, E.M. Sparrow, The effect of superheating on condensation heat transfer in a forced convection boundary layer flow, Int. J. Heat Mass Transfer 12 (1969) 147–154.
[3] J. Mitrovic, Effect of vapor superheat and condensate subcooling on laminar film condensation, ASME J. Heat Transfer 122 (2000) 192–196.
[4] R.L. Webb, Convective condensation of superheated vapor, ASME J. Heat Transfer 120 (1998) 418–421.
[5] M. Goto, H. Hotta, S. Tezuka, Film condensation of refrigerant vapours on a horizontal tube, Int. J. Refrig. 3 (1980) 161–166.
[6] W.W. Huebsch, M.B. Pate, Heat Transfer Evaluation of HFC-236ea and CFC-114 in Condensation and Evaporation, EPA/60/SR-96/070, 1996.
[7] G.A. Longo, Refrigerant R134a condensation heat transfer and pressure drop inside a small brazed plate heat exchanger, Int. J. Refrig. 31 (2008) 780–789.
[8] G.A. Longo, R410A condensation inside a commercial brazed plate heat exchanger, Exp. Therm. Fluid Sci. 33 (2009) 284–291.
[9] R.K. Shah, W.W. Focke, Plate heat exchangers and their design theory, in: R.K. Shah, E.C. Subbarao, R.A. Mashelkar (Eds.), Heat Transfer Equipment Design, Hemisphere, Washington, 1988, pp. 227–254.
[10] K.J. Bell, Temperature profiles in condensers, Chem. Eng. Prog. 68 (1972) 81–82.
[11] K.J. Bell, A.C. Mueller, Condensing Heat Transfer, Wolverine Heat Transfer Data Book, Wolverine, 1984.
[12] A. Muley, R.M. Manglik, Experimental study of turbulent flow heat transfer and pressure drop in a plate heat exchanger with chevron plates, ASME J. Heat Transfer 121 (1999) 110–121.
[13] G.A. Longo, A. Gasparella, Heat transfer and pressure drop during HFC refrigerant vaporisation inside a brazed plate heat exchanger, Int. J. Heat Mass Transfer 50 (2007) 5194–5203.
[14] NIST, Refrigerant Properties Computer Code, REFPROP 7.0, 2002.
[15] B. Palm, J. Claessson, Plate heat exchangers: calculation methods for single- and two-phase flow, Heat Transfer Eng. 27 (2006) 88–98.
[16] S.J. Kline, F.A. McClintock, Describing uncertainties in single-sample experiments, Mech. Eng. 75 (1953) 3–8.
[17] G.A. Longo, Heat transfer and pressure drop during hydrocarbon refrigerant condensation inside a brazed plate heat exchanger, Int. J. Refrig. 33 (2010) 944–953.
[18] W.W. Akers, H.A. Deans, O.K. Crosser, Condensing heat transfer within horizontal tubes, Chem. Eng. Prog. Symp. Ser. 55 (1959) 171–176.
[19] Z.H. Ayub, Plate heat exchanger literature survey and new heat transfer and pressure drop correlations for refrigerant evaporators, Heat Transfer Eng. 24 (2003) 3–16.